

COMPUTATIONAL SIMULATION OF CANCELLOUS BONE REMODELING USING DIGITAL IMAGE-BASED MODEL

Ken-ichi TSUBOTA^{*}, Taiji ADACHI[†], and Yoshihiro TOMITA[#]

Graduate School of Science and Technology, Kobe University
1-1 Rokkodai, Nada, Kobe 657-8501, Japan

RIKEN
2-1 Hirosawa, Wako-shi, Saitama 351-0198, Japan

^{*} e-mail: tsubota@solid.mech.kobe-u.ac.jp

[†] e-mail: adachi@mech.kobe-u.ac.jp

[#] e-mail: tomita@mech.kobe-u.ac.jp

Abstract. *A computational simulation method for trabecular surface remodeling in cancellous bone was proposed using a digital image-based voxel finite element model. For cancellous bone with complicated trabecular architecture, digital image-based model is useful both for finite element modeling of the structure and for simulating morphological changes in the trabecular architecture due to remodeling. Trabecular surface remodeling was simulated based on a uniform stress hypothesis, that is, to attain uniform stress in the trabeculae, resorption and formation were modeled by removal and addition of the voxel finite elements on the trabecular surface. A remodeling simulation of a cancellous bone cube under compressive loading was conducted with a digital image-based model constructed from μ CT data of the cancellous region in a distal canine femur. The results of the simulation demonstrate that the trabeculae change their morphology to functionally adapt to the applied load as a load-bearing structure, and the changes in the structural indices of cancellous bone qualitatively correspond with the experimental results, demonstrating the potential of the proposed method to predict the functional adaptation of cancellous bone.*

1. INTRODUCTION

The trabecular architecture of cancellous bone changes and is maintained by adaptive remodeling, in which morphological changes in the trabeculae result from coupled osteoclastic resorption and osteoblastic formation on the trabecular surface. Recent advances in understanding the mechanical adaptation of bone by remodeling have benefited from a computational mechanics approach that allows an analysis of the structural and functional changes in bone under complicated mechanical conditions (Cowin, 1993; Huijkes and Hollister, 1993). Theoretical modeling and computational simulation of bone remodeling originated in continuum and computational mechanics (Cowin and Hegedus, 1976; Hart *et al.*, 1984; Carter *et al.*, 1987; Huijkes *et al.*, 1987; Beaupré *et al.*, 1990; Weinans *et al.*, 1992), in which remodeling rate equations were proposed for cortical and cancellous bone as a continuum. Recently, however, it has been recognized that isotropic continuum modeling and simulation have limitations in the sense that anisotropy of the

mechanical properties is essential to bone mechanics, and the local mechanical stimuli at the microstructural level affect the cellular activities in the remodeling process (Cowin *et al.*, 1991; Guldborg *et al.*, 1997). To account for trabecular level adaptation, both theoretical models and computational simulations have been overlapped and developed (Cowin *et al.*, 1992; Sadegh *et al.*, 1993; Mullender *et al.*, 1994; Adachi *et al.*, 1999).

For the computational modeling of bone with a complex microstructure, digital image-based voxel models of cancellous bone with a high resolution have been available since the introduction of imaging and quantifying techniques for the trabecular bone architecture in three dimensions, such as the micro-computed tomography (μ CT) scanning technique (Feldkamp *et al.*, 1989). These techniques enabled calculation of trabecular bone apparent mechanical properties using a homogenization procedure and direct estimation of the stress and strain at the trabecular level (Hollister *et al.*, 1994; Van Rietbergen *et al.*, 1995) that regulate the cellular activities in bone remodeling. These techniques can also be applied to quantify changes in the trabecular architecture of cancellous bone from *in vivo* animal experiments under controlled mechanical conditions (Goldstein *et al.*, 1991; Guldborg *et al.*, 1997). Establishing a computational simulation method for trabecular bone remodeling by using digital image-based voxel finite element models and applying this technique complementarily with experimental observations would therefore be a powerful tool for clarifying the mechanism for the adaptive bone remodeling.

The purposes of this study are to propose a simulation method for the three-dimensional trabecular surface remodeling of cancellous bone by using digital image-based voxel finite element models, and to demonstrate the feasibility of the proposed method through the simulation studies on a cancellous bone cube under compressive loading. First, the rate equation for trabecular surface remodeling (Adachi *et al.*, 1997) based on the uniform stress hypothesis (Adachi *et al.*, 1998) is summarized. Second, this remodeling rate equation is applied to voxel finite element models of trabecular bone. Third, a remodeling simulation is carried out on a cancellous bone cube that was obtained from the cancellous region of a canine distal femur by using three-dimensionally reconstructed μ CT data (Goldstein *et al.*, 1991; Guldborg *et al.*, 1997) under uniaxial compressive loading. The results obtained in the simulation are examined in the context of functional adaptation by remodeling as a load-bearing structure, and the applicability of the simulation method to predict actual trabecular remodeling phenomena is evaluated by a comparison with the experimental results.

2. MODEL FOR TRABECULAR SURFACE REMODELING

2.1 Resorption and Formation on a Trabecular Surface

The trabecular microstructure of cancellous bone changes under the influence of mechanical factors due to locally regulated cellular activities on the trabecular surface. This trabecular surface remodeling has a cycle with five successive stages of quiescence, activation, osteoclastic resorption, reversal and osteoblastic formation (Parfitt, 1994), as illustrated in Fig.1(a), that is called remodeling turnover. The relative difference in amount between the downward erosion by resorption and the upward cavity refilling by formation, moving in a direction perpendicular to the trabecular surface, determines the local movement of the trabecular surface.

Due to the cyclical nature of the remodeling turnover process, the rate equation for trabecular surface remodeling should be considered in two different hierarchical time scales,

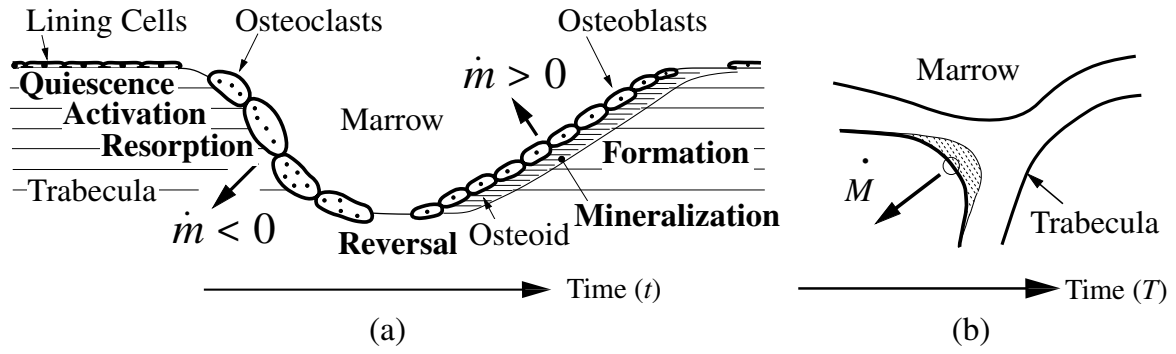


Figure 1: Trabecular surface remodeling by cellular activity: (a) Osteoclastic resorption and osteoblastic formation on a trabecular surface (time scale t); (b) Surface movement by trabecular surface remodeling (time scale T)

t and T , as is shown in Fig.1. One time scale t is for the cellular activity describing remodeling turnover (Fig.1(a)), and the other time scale T is a longer scale than that for the characteristic period of remodeling turnover (Fig.1(b)). It should be noted that the first time scale t is considered long enough when compared to the time scale τ that measures the dynamic changes due to body motion.

Let \dot{m} denote the rate of surface movement by remodeling in the outer direction perpendicular to the trabecular surface: $\dot{m}=0$ (quiescence), $\dot{m}<0$ (resorption), and $\dot{m}>0$ (formation). Averaging \dot{m} over the characteristic period of the remodeling cycle, the rate of trabecular surface remodeling, \dot{M} , is defined on the time scale T . In the following sections, the expression of \dot{M} is discussed for trabecular surface remodeling as a local stress regulation process.

2.2 Driving Force for Trabecular Surface Remodeling

Regulation of the cellular events responsible for remodeling turnover is systematically and locally controlled in the bone macro- and micro-environment: i.e., systematic regulation by hormones, and local regulation by growth factors and cytokines (Baylink *et al.*, 1993; Manolagas, 1995). It has also been experimentally revealed that local mechanical signals play an important role in trabecular bone remodeling (Guldberg *et al.*, 1997). We have assumed that systematic regulation is related to changes in the amount of bone measured by the volume fraction, and that local mechanical regulation is related to morphological changes in the trabecular architecture.

To discuss how the regulation of a microscopic mechanical stimulus is related to local trabecular surface remodeling and how the macroscopic trabecular architecture emerges from the local morphological changes due to trabecular surface remodeling, we use the local stress as the mechanical stimulus regulating trabecular surface remodeling. As a simple case, we consider positive scalar function σ as a mechanical stimulus to be employed in the rate equation for trabecular surface remodeling. Based on the hypothesis that the mechanical stimulus becomes uniform at the remodeling equilibrium state as a result of functional adaptation (Fung, 1984; Takamizawa and Hayashi, 1987; Adachi *et al.*, 1998), we assume the nonuniformity of the mechanical stimulus σ as a driving force for remodeling to seek the uniform state.

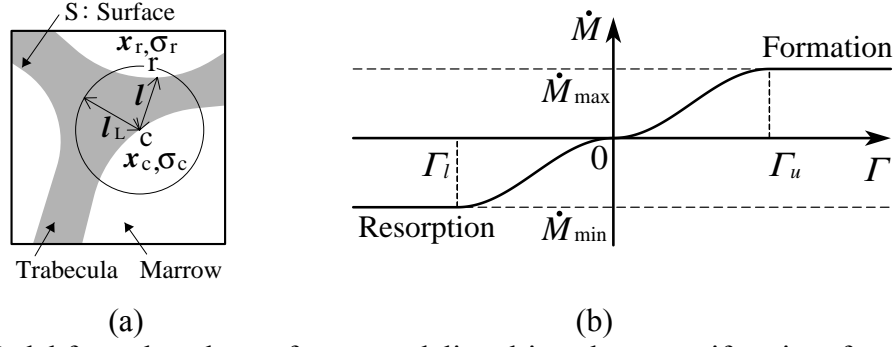


Figure 2: Model for trabecular surface remodeling driven by nonuniformity of mechanical stimulus on the trabecular surface: (a) The driving force for the remodeling Γ is defined as the relative difference between stress σ_c at x_c and σ_d at the neighboring point ($l < l_L$); (b) Remodeling rate equation as a function of the driving force for the remodeling Γ .

To express nonuniformity of the scalar function of mechanical stimulus σ in space, the integral form with weight function can be used. By averaging $\sigma_r(x_r)$ at neighbor point x_r with weight function $w(l)$, as illustrated in Fig.2(a), representative neighbor stress $\sigma_d(x_c)$ at x_c is determined as

$$\sigma_d = \int_S w(l) \sigma_r dS / \int_S w(l) dS, \quad (1)$$

where S denotes the trabecular surface, $l = |x_r - x_c|$, and weight function $w(l)$ takes a non-zero positive value at neighbor point ($l < l_L$). This expression of Eq.(1) can be extended to consider the nonuniformity of stress in the trabeculae by integrating over volume element dV for the case in which the role of the osteocyte (Cowin *et al.*, 1991) is taken into account.

As the driving force for local trabecular remodeling, we use the relative value of the stress σ_c at x_c to σ_d at x_c that is defined as

$$\Gamma(x_c) = \ln(\sigma_c / \sigma_d). \quad (2)$$

This function Γ expresses the convexity of the stress distribution, taking a positive value with a convex stress distribution and a negative one with a concave distribution. The weight function, $w(l) : w(l) > 0 (0 \leq l < l_L)$ and $w(l) = 0 (l_L \leq l)$, in Eq.(1) is a monotonously decreasing function with respect to distance l , that determines the size of the region ($l < l_L$) in which the mechanical stimulus affects the remodeling at point x_c . Thus, estimating the representative stress σ_d at the neighbor point by using the integral form of Eq.(1) takes into account the existence of the sensory network between cells (Donahue *et al.*, 1995).

2.3 Rate Equation for Trabecular Surface Remodeling

In general, an addition of material to the surface of a structural component reduces the stress on its surface, and removal induces a higher stress. Thus, by using driving force Γ in Eq.(2), the remodeling rate equation is generally written as

$$\dot{M} = F(\Gamma) = \begin{cases} \Gamma > 0 : \text{Formation} \\ \Gamma < 0 : \text{Resorption} \end{cases} \quad (3)$$

to express formation at a site with convex distribution of σ and resorption at a site with a concave distribution of σ , where function F determines the features of the rate equation.

As a simple case, function F in Fig.2(b) is used in this study, in which parameters Γ_u and Γ_l are the upper and lower threshold values, respectively. Regions $\Gamma_l \leq \Gamma \leq 0$ and $0 \leq \Gamma \leq \Gamma_u$ are interpolated by sine functions. As remodeling progresses, the nonuniformity in surface stress becomes smaller, that is, $|\Gamma|$ approaches zero within the lazy zone of remodeling (Huiskes *et al.*, 1987) around the equilibrium point, $\dot{M} = 0$, as shown in Fig.2(b). Two model parameters are introduced in the rate equation to express spatial and time effects. The parameter, l_L , in Fig.2(a) regulates the spatial sensitivity that represents the area where cells can sense a mechanical stimulus. As a result, l_L regulates the spatial distribution of the trabecular apparent density, which plays the role of a spatially sensitive parameter. The other parameters, Γ_u and Γ_l , in Fig.2(b) affect the rate of volumetric change in time, which play the role of remodeling rate-sensitive parameters.

In this equation, the local remodeling rate is determined by using only a local mechanical stimulus evaluated by Γ without using any systematic global stresses prescribed *a priori*, such as goal or optimal stresses. This model can be extended to consider remodeling in response to a change in stress magnitude in time without changing the stress distribution pattern (Tanaka *et al.*, 1993).

3. VOXEL SIMULATION MODEL FOR TRABECULAR SURFACE REMODELING

3.1 Voxel Finite Element Discretization of Cancellous Bone

A voxel finite element model of trabeculae (Hollister and Kikuchi, 1994; Hollister *et al.*, 1994; Van Rietbergen *et al.*, 1995; Ulrich *et al.*, 1998) can be reconstructed from digital images such as those obtained by μ CT scanning (Feldkamp *et al.*, 1989) and be used to represent the trabecular architecture in detail. In this study, the proposed model for trabecular surface remodeling was applied to voxel finite element models of the trabecular architecture in cancellous bone, combining these with the solver for a large-scale finite element model.

The trabecular architecture in a three-dimensional region was discretized by using voxel finite elements with regular mesh divisions as shown in Fig.3(a). Thus, the trabeculae were modeled as an assemblage of voxel finite elements, and morphological changes were accomplished by removing/adding elements from/to the trabecular surface in response to the mechanical stimulus calculated by the finite element analysis. Each element size should be

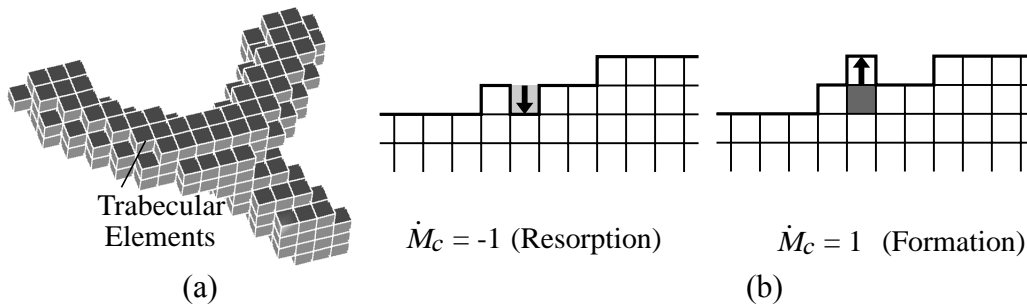


Figure 3: Voxel simulation model of trabecular surface remodeling: (a) Voxel finite element discretization of the trabeculae; (b) Surface movement due to formation and resorption on trabeculae represented by addition and removal of voxel finite element.

smaller than the dimensions of the basic multi-cellular unit (Parfitt, 1994) for remodeling, so that the trabecular diameter was discretized into at least 3 elements as an initial shape in the remodeling simulation.

In the three-dimensional finite element analysis, the trabecular bone part was assumed to be a homogeneous and isotropic elastic material with Young's modulus of $E = 20$ GPa and Poisson's ratio of $\nu = 0.3$, the marrow part being excluded as a cavity. Since the trabeculae were discretized by regular voxel elements, an iterative equation solver called the element-by-element preconditioned conjugate gradient (EBE/PCG) method (Hughes *et al.*, 1987; Van Rietbergen *et al.*, 1995) with diagonal scaling was used for a large-scale finite element analysis.

3.2 Simulation Procedure for Trabecular Surface Remodeling

The simulation of trabecular surface remodeling with microstructural voxel finite element models was carried out by the following procedure:

- (1) Discretize the initial shape of the trabecular architecture in the region being analyzed.
- (2) Analyze stress σ in the trabecular elements by a finite element procedure with the EBE/PCG method under given boundary conditions.
- (3) Evaluate the surface stress nonuniformity Γ for all trabecular surface elements.
- (4) Determine the rate of surface movement \dot{M} , and remove/add the surface voxel element.
- (5) If remodeling equilibrium is not attained, repeat the procedure from step (2).

Procedures (2) to (5) are one step of the simulation. In this study, the equivalent stress is used as scalar function σ of the stress. If other positive values, such as the strain energy density, are used as a mechanical stimulus, similar results can be expected at the equilibrium state (Adachi *et al.*, 1997).

4. REMODELING OF CANCELLOUS BONE UNDER COMPRESSIVE LOADING

4.1 Digital Image-based Model of Cancellous Bone

A digital image-based model of a cancellous bone cube of $a = 5$ mm on each side was obtained from a canine distal femoral metaphyses, to which a hydraulically controlled load was applied via platens of 6mm in diameter (Goldstein *et al.*, 1991; Guldberg *et al.*, 1997), based on three-dimensionally reconstructed μ CT data as shown in Fig.4(a). Each voxel size was $25 \mu\text{m}$ to give the same resolution as the μ CT data, so that the total volume contained $200^3 = 8$ million voxel elements of which about 2.3 million were trabecular bone elements.

The structural indices of the trabecular architecture (Feldkamp *et al.*, 1989), which could be directly calculated from the binarized three-dimensional data, were the bone volume fraction $BVF = 0.282$, trabecular plate thickness $TPT = 112 \mu\text{m}$, trabecular plate number $TPN = 2.52 \text{ mm}^{-1}$, and trabecular plate separation $TPS = 286 \mu\text{m}$. The fabric ellipsoid of the trabecular architecture (Cowin, 1985) and the middle $\tilde{X}_1\tilde{X}_3$ cross section are shown in Fig.4(a) in which the principal values $H_i (i = 1, 2, 3; H_1 \geq H_2 \geq H_3)$ are $H_1 = 387 \mu\text{m}$, $H_2 = 311 \mu\text{m}$, and $H_3 = 291 \mu\text{m}$; and angle Θ_{i3} between principal direction n_i and compressive axis X_3 are $\Theta_{13} = 73.6^\circ$, $\Theta_{23} = 37.0^\circ$, and $\Theta_{33} = 57.9^\circ$. Thus, the degree of anisotropy of the initial trabecular bone model was $H_1/H_3 = 1.33$, and the direction of anisotropy was relatively close to the perpendicular to the X_3 coordinate axis.

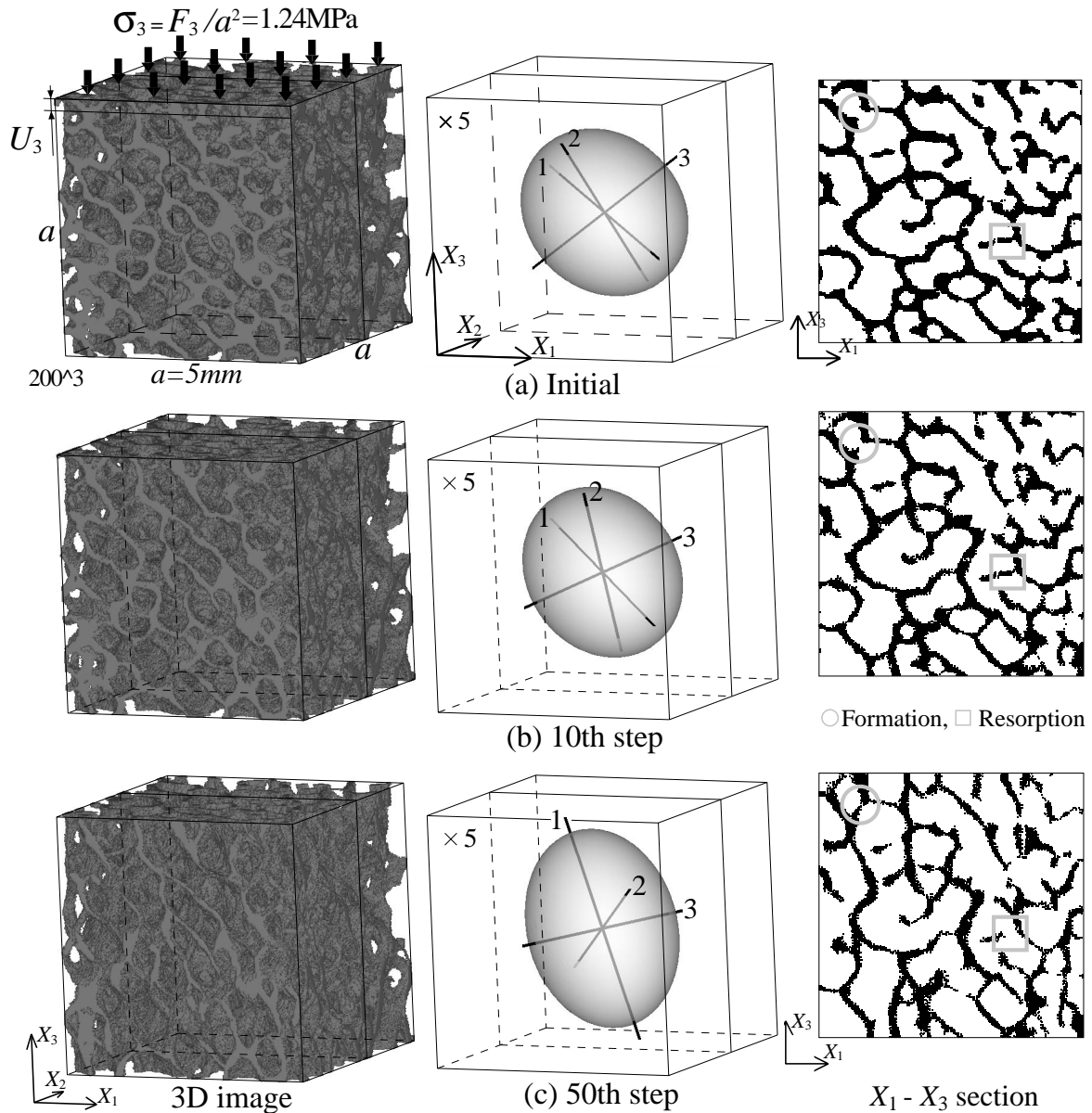


Figure 4: Remodeling simulation of cancellous bone under compressive loading by using μ CT image-based voxel finite element models obtained from a canine distal femur. 3D image (200^3 voxels), fabric ellipsoid, and $X_1 - X_3$ cross section: (a) Initial; (b) 10th step; (c) 50th step.

As boundary conditions, uniform displacement $U_3 (< 0)$ was controlled at every simulation step on the upper plane at $X_3 = 5.0$ mm to apply an average stress of $\sigma_3 = F_3/a^2 = -1.24$ MPa by referring to the experimental value (Guldberg *et al.*, 1997), as shown in Fig.4(a), where $F_3 (< 0)$ was the total force applied on the plane and $\epsilon_3 = U_3/a$ is defined as the apparent strain in the X_3 direction. On the other five planes, shear-free boundary conditions were applied, that is, the displacement perpendicular to each of these

planes was fixed. Sensing distance l_L in weight function $w(l)$ was set to $500\mu\text{m}$, this being equal to the length of 20 voxel elements, and the threshold values for remodeling were set to $\Gamma_u = 4.0$ and $\Gamma_l = -5.0$. These model parameters should be determined from a comparison with the experimental observations (Tsubota *et al.*, 2000).

4.2 Remodeling at the Trabecular Structural Level

The morphological changes in the trabecular architecture of the cancellous bone cube due to remodeling under a compressive load at the 10th and 50th steps are presented in Figs.4(b) and (c), in which fabric ellipsoids of the three-dimensional architecture and X_1 - X_3 cross section show the development of trabecular anisotropy. The initial morphology shown in Fig.4(a) adapted to the applied compressive loading by resorption and formation on the trabecular surface to reduce the nonuniformity of the stress. The degree of anisotropy defined as H_1/H_3 increased from 1.33 (initial) to 1.39 (50th step) by aligning the trabecular architecture along the compressive loading axis which can be observed by the rotation of the principal direction of the fabric ellipsoid from Fig.4(a) to (c). Preferential loss of the horizontal trabeculae, marked by open rectangles in the cross-sectional image in Fig.4, and preservation and increase in thickness of the vertically oriented trabeculae directed along the compressive loading axis, marked by open circles, contributed to the development of this trabecular anisotropy.

Changes in structural indices are plotted in Figs.5(a) and (b), where the indices were measured by using voxel finite elements at every simulation step for the center core cube of $4.0\times 4.0\times 4.0\text{mm}$ to eliminate numerical errors adjacent to the boundary in the remodeling simulation. As a result of the remodeling, a decrease of 21.2% in the bone volume fraction (*BVF*), a 19.3% decrease in the trabecular plate thickness (*TPT*), and a 2.2% decrease in the trabecular plate number (*TPN*) were found at the 50th step when compared with the initial values, which resulted in a 10.0% increase in the trabecular plate separation (*TPS*). This increase in *TPS* occurred because resorption of the horizontal trabeculae was more marked than the formation of the vertical trabeculae. The angle θ_{i3} between the principal directions n_i of the fabric ellipsoid and the loading axis X_3 changed by reorientation of the trabecular architecture, as shown in Fig.5(c). The angle θ_{13} monotonously decreased from 73.6° toward zero, while θ_{23} and θ_{33} increased toward 90° . These changes in structural index and angle indicate that the trabecular orientation was changed to align with the compressive axis X_3 , showing adaptive remodeling to support the uniaxial compressive loading. To investigate the functional changes in the trabecular architecture as a load-bearing structure due to remodeling, the apparent stiffness of the core cube of $4.0\times 4.0\times 4.0\text{mm}$ in the three orthogonal axes of X_1 , X_2 , and X_3 were numerically measured by uniaxial compression testing at each simulation step. The applied boundary conditions were similar to those for the remodeling simulation, with uniform displacement being applied on the upper surface, and the other surfaces being fixed with stress-free conditions. Changes in apparent stiffness σ_i/ε_i in the directions of the coordinate axes X_i are plotted in Fig.5(d). In the compressive loading direction for the remodeling simulation, X_3 direction, the apparent stiffness σ_3/ε_3 gradually increased by 29.4%; however, both σ_1/ε_1 and σ_2/ε_2 in the direction perpendicular to the loading axis decreased by about 60% due to remodeling. Thus, remodeling resulted in functional changes in the trabecular architecture, and increased the degree of anisotropy of the mechanical properties. Even though the average bone volume

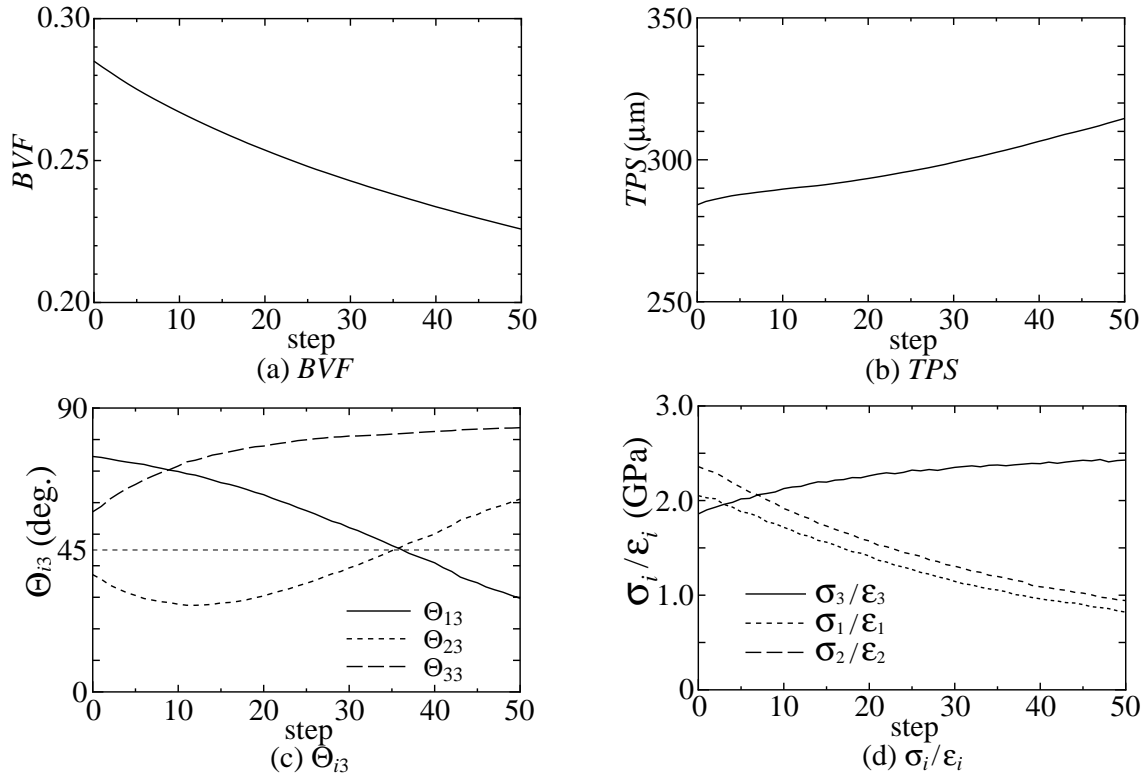


Figure 5: Changes in structural indices, principal direction of trabecular architecture and apparent stiffness of cancellous bone due to remodeling under compressive loading: (a) bone volume fraction; (b) trabecular plate separation; (c) angle Θ_{i3} between the principal direction of H_i and loading axis X_3 ; and (d) apparent stiffness σ_i/ϵ_i in X_i direction

fraction was decreased by remodeling as shown in Fig.5(a), the structural stiffness was increased by remodeling as shown in Fig.5(d), thus demonstrating the adaptive response to support compressive loading by reorganizing the trabecular architecture.

5. DISCUSSION

Driven by the nonuniformity of the stress, adaptive reorganization of the trabecular architecture by remodeling could be smoothly simulated, as shown in Figs.4 and 5, and a uniform stress distribution was accomplished by using digital image-based voxel finite element models. This result has demonstrated that the proposed voxel simulation method was applicable to approximate the model for trabecular surface remodeling at the trabecular structural level. The apparent stiffness along the compressive loading axis increased by reorganizing the trabecular architecture and by increasing the degree of anisotropy, although the volume fraction decreased. This result implies that remodeling under the assumption of the uniform stress hypothesis revealed the functional adaptive response of the bone as a load-bearing structure. We thus demonstrated that the proposed model for trabecular surface remodeling and its simulation method of using voxel finite element models were applicable to simulate the functional adaptation phenomenon in cancellous bone remodeling.

To quantitatively evaluate the simulation results, a comparison with the experimental results is necessary. In the experiment (Guldberg *et al.*, 1997) using a canine model that was capable of applying a hydraulically controlled load to the distal femoral cancellous bone, trabecular structural changes due to remodeling in experimental side were compared with the control side. In this simulation, the initial digital image-based model was produced with reference to the control trabecular bone cube, so that the simulated results correspond with those for the experimental trabecular bone. Structural indices for the control and experimental bones for one canine and the simulated results are listed in Table 1. In this simulation, the trabecular bone volume (BVF), trabecular plate number (TPN) and angle Θ_{13} of the principal axis of the trabecular architecture each decreased, while the trabecular plate separation (TPS) increased by remodeling under compressive loading. These results qualitatively match the experimental observations, in which changes in BVF , TPN , Θ_{13} , and TPS were statistically significant when compared with the control data in the experiment. The simulated result for trabecular plate thickness (TPT) showed a decrease by remodeling, while the experimental TPT did not show significant change. This was due to the fact that the comparison between the experimental and simulated data in Table 1 was done for only one set of canine data. The discrepancy between the experimental and simulated results could have been due to approximated boundary conditions, unknown model parameters, or unknown *in vivo* biological factors in the system. To develop models that can predict details of the remodeling phenomenon, model parameters Γ_u , Γ_l , and l_L have to be quantitatively determined by a comparison with the experimental observations (Tsubota *et al.*, 2000).

Table 1: Structural indices and principal direction of trabecular architecture for the control, experiment, and simulation

	BVF	TPT (μm)	TPN (mm^{-1})	TPS (μm)	Θ_{13} (deg.)
Control	0.282	112	2.52	286	73.6
Experiment	0.230	121	1.88	421	47.9
Simulation	0.222	90	2.47	317	31.9

One of the most remarkable features of the proposed simulation method is its capability to handle the large-scale three-dimensional voxel model with a regular finite element mesh for the complex trabecular architecture. This offers many practical advantages in that it enables us to make voxel finite element models based on digital images such as those obtained by using μCT , and that a variety of cancellous bone samples can be analyzed by using images provided from an *in vivo* experiment. It is also easy to apply linear solvers such as the EBE/PCG method to the large-scale three-dimensional models. Furthermore, this simulation method could be utilized as a tool to visualize the morphological change in trabecular architecture due to remodeling in a computer. This technique will therefore be useful for further elucidation of the trabecular bone-remodeling phenomenon by directly observing the microscopic structural change with the proposed simulation.

6. CONCLUSIONS

A computational simulation method for trabecular surface remodeling has been proposed by using voxel finite element models of cancellous bone with a trabecular microstructure. This method was applied to simulate remodeling of trabeculae under compressive loading at the trabecular structural level. Since trabeculae with a complex three-dimensional architecture were modeled as an assemblage of regular voxel elements, morphological changes were directly accomplished by removing and adding elements on the trabecular surface, and EBE/PCG method for large-scale computation was applicable.

The cancellous bone cube for the simulation was modeled based on digital images obtained by μ CT and compressed under uniaxial loading. The trabeculae perpendicular to the loading direction became thinner, and those along the axis became thicker by remodeling to obtain a uniform stress distribution. The resulting reorientation of the trabecula to the compressive loading direction and the increase in the degree of anisotropy increased the apparent stiffness against the loading, even though the volume fraction was decreased by remodeling. Changes in the structural indices of the trabecular architecture by remodeling qualitatively matched the experimental observations (Guldberg *et al.*, 1997).

The results of these studies enable us to conclude that the proposed remodeling rate equation and simulation method using digital image-based voxel finite element model could be applicable to predict actual trabecular remodeling phenomena such as the adaptive response around artificial prostheses and implants. A quantitative comparison of the changes in structural indices with the experimental results obtained under a controlled mechanical environment would enable us to develop more detailed models.

Application of this simulation method to bone tissue engineering would be an exciting challenge, with the application to optimal design of the biomaterial scaffold for regenerating bone tissue (Hollister *et al.*, 1999). This method could be applied to design the scaffold topology and pore geometry that considers the bone mechanical properties as an initial load support, fluid diffusion through the scaffold pore and deformation controlling biological cellular activities. It could also be utilized to design the optimal combination between degradation of the biomaterial scaffold and newly developed bone by adaptive ingrowth and formation. When combined with a sophisticated measuring system for the bone microstructure such as μ CT, the proposed simulation method is expected to have potential for constructing a new design system for the scaffold for use in bone tissue engineering.

ACKNOWLEDGMENTS

The authors thank Steve Goldstein, Scott Hollister and Nancy Caldwell of the Orthopaedic Research Laboratories at the University of Michigan for the digital image data of cancellous bone and for helpful comments.

REFERENCES

- Adachi, T., Tomita, Y., Sakaue, H., and Tanaka, M., 1997, Simulation of Trabecular Surface Remodeling Based on Local Stress Nonuniformity, *JSME Int. J.*, Vol. 40C, No. 4, pp. 782-792.
- Adachi, T., Tanaka, M., and Tomita, Y., 1998, Uniform Stress State in Bone Structure with

- Residual Stress, *Trans. ASME, J. Biomech. Eng.*, Vol. 120, No. 3, pp. 342-347.
- Adachi, T., Tomita, Y., and Tanaka, M., 1999, Three-Dimensional Lattice Continuum Model of Cancellous Bone for Structural and Remodeling Simulation, *JSME Int. J.*, Vol. 42C, No.3, pp. 470-480.
- Baylink, D. J., Finkelman, R. D., and Mohan, S., 1993, Growth Factors to Stimulate Bone Formation, *J. Bone & Mineral Res.*, Vol. 8, No. S2, pp. S565-S572.
- Beaupré, G. S., Orr, T. E., and Carter, D. R., 1990, An Approach for Time-dependent Bone Modeling and Remodeling: Theoretical Development, *J. Orthop. Res.*, Vol. 8, pp. 651-661.
- Carter, D. R., Fyhrie, D. P., and Whalen, R. T., 1987, Trabecular Bone Density and Loading History: Regulation of Connective Tissue Biology by Mechanical Energy, *J. Biomech.*, Vol. 20, No. 8, pp. 785-794.
- Cowin, S. C. and Hegedus, D. H., 1976, Bone Remodeling I: A Theory of Adaptive Elasticity, *J. Elasticity*, Vol. 6, No.3, pp. 313-326.
- Cowin, S. C., 1985, The Relationship between the Elasticity Tensor and the Fabric Tensor, *Mechanics of Materials*, Vol. 4, pp. 137-147.
- Cowin, S. C., Moss-Salentijn, L., and Moss, M. L., 1991, Candidates for the Mechanosensory System in Bone, *Trans. ASME, J. Biomech. Eng.*, Vol. 113, No. 2, pp. 191-197.
- Cowin, S. C., Sadegh, A. M., and Luo, G. M., 1992, An Evolutionary Wolff's Law for Trabecular Architecture, *Trans. ASME, J. Biomech. Eng.*, Vol. 114, No.1, pp.129-136.
- Cowin, S. C., 1993, Bone Stress Adaptation Models, *Trans. ASME, J. Biomech. Eng.*, Vol. 115, No. 4B, pp. 528-533.
- Donahue, H. J., McLeod, K. J., Rubin, C. T., Andersen, J., Grine, E. A., Hertzberg, E. L., and Brink, P. R., 1995, Cell-to-Cell Communication in Osteoblastic Networks: Cell Line-Dependent Hormonal Regulation of Gap Junction Function, *J. Bone & Mineral Res.*, Vol. 10, No. 6, pp. 881-889.
- Feldkamp, L. A., Goldstein, S. A., Parfitt, A. M., Jesion, G., and Kleerekoper, M., 1989, The Direct Examination of Three-Dimensional Bone Architecture *In Vitro* by Computed Tomography, *J. Bone & Min. Res.*, Vol. 4, No. 1, pp. 3-11.
- Fung, Y. C., 1984, In: *Biodynamics: Circulation*, pp. 64, Springer.
- Goldstein, S. A., Matthews, L. S., Kuhn, J. L., and Hollister, S. J., 1991, Trabecular Bone Remodeling: An Experimental Model, *J. Biomech.*, Vol. 24, Suppl. 1, pp. 135-150.
- Guldberg, R. E., Richards, M., Caldwell, N. J., Kuelske, C. L., and Goldstein, S. A., 1997, Trabecular Bone Adaptation to Variations in Porous-Coated Implant Topology, *J. Biomech.*, Vol. 30, No. 2, pp. 147-153.
- Hart, R. T., Davy, D. T., and Heiple, K. G., 1984, A Computational Method for Stress Analysis of Adaptive Elastic Materials with a View toward Applications in Strain-induced Bone Remodeling, *Trans. ASME. J. Biomech. Eng.*, Vol. 106, No.4, pp. 342-350.
- Hollister, S. J. and Kikuchi, N., 1994, "Homogenization Theory and Digital Imaging: A Basis for Studying the Mechanics and Design Principles of Bone Tissue," *Biotech. & Bioeng.*, Vol. 43, pp. 586-596.
- Hollister, S. J., Brennan, J. M., and Kikuchi, N., 1994, A Homogenization Sampling Procedure for Calculating Trabecular Bone Effective Stiffness and Tissue-Level Stress, *J. Biomech.*, Vol. 27, No.4, pp. 433-444.
- Hollister, S. J., Chu, T. M., Guldberg, R. E., Zysset, P. K., Levy, R. A., Halloran, J. W., and Feinberg, S. E., 1999, Image Based Design and Manufacture of Scaffolds for Bone Reconstruction, In: *Synthesis in Bio Solid Mechanics*, (Eds: Pedersen, P. and Bendsoe, M.

- P.), pp. 163-174, Kluwer Academic Publishers.
- Hughes, T. J. R., Ferencz, R. M., and Hallquist, J. O., 1987, Large-Scale Vectorized Implicit Calculations in Solid Mechanics on a Cray X-MP/48 Utilizing EBE Preconditioned Conjugate Gradients, *Comp. Methods Appl. Mech. Eng.*, Vol. 61, pp. 215-248.
- Huiskes, R., Weinans, H., Grootenboer, H. J., Dalstra, M., Fudala, B., and Slooff, T. F., 1987, Adaptive Bone-Remodeling Theory Applied to Prosthetic-Design Analysis, *J. Biomech.*, Vol. 10, No. 11/12, pp. 1135-1150.
- Huiskes, R. and Hollister, S. J., 1993, From Structure to Process, From Organ to Cell: Recent Developments of FE-Analysis in Orthopaedic Biomechanics, *Trans. ASME, J. Biomech. Eng.*, Vol. 115, No. 4B, pp. 520-527.
- Manolagas, S. C., 1995, Role of Cytokines in Bone Resorption, *Bone*, Vol. 17, No. 2, pp. 63S-67S.
- Mullender, M. G., Huiskes, R., and Weinans, H., 1994, A Physiological Approach to the Simulation of Bone Remodeling as a Self Organization Control Process, *J. Biomech.*, Vol. 27, No. 11, pp. 1389-1394.
- Mundy, G. R., 1999, Cellular and Molecular Regulation of Bone Turnover, *Bone*, Vol. 24, No. 5S, pp. 35S-38S.
- Parfitt, A. M., 1994, Osteonal and Hemi-Osteonal Remodeling: The Spatial and Temporal Framework for Signal Traffic in Adult Human Bone, *J. Cellular Biochem.*, Vol. 55, pp. 273-286.
- Sadegh, A. M., Luo, G. M., and Cowin, S. C., 1993, Bone Ingrowth: An Application of the Boundary Element Method to Bone Remodeling at the Implant Interface, *J. Biomech.*, Vol. 26, No. 2, pp. 167-182.
- Takamizawa, K. and Hayashi, K., 1987, Strain Energy Density Function and Uniform Strain Hypothesis for Arterial Mechanics, *J. Biomech.*, Vol. 20, No. 1, pp. 7-17.
- Tanaka, M., Adachi, T., and Tomita, Y., 1993, Bone Remodeling Considering Residual Stress: Preliminary Experimental Observation and Theoretical Model Development, In: *Computational Biomedicine* (Eds: Heldm, D. K., Brebbia, C. A., Ciskowski, R. D., and Power, H.), pp. 239-246, Computational Mechanics Publications, Southampton Boston.
- Tsubota K., Adachi, T., and Tomita, Y., 2000, Simulation Study on Model Parameters of Trabecular Surface Remodeling Model, In: *Proc. 4th Int. Symp. on Comp. Meth. in Biomech. & Biomed. Eng.*, (in press).
- Ulrich, D., Van Rietbergen, B., Weinans, h., and Ruegsegger, P., 1998, Finite Element Analysis of Trabecular Bone Structure: A Comparison of Image-based Meshing Techniques, *J. Biomech.*, Vol. 31, No. 12, pp. 1187-1192.
- Van Rietbergen, B., Weinans, H., Huiskes, R., and Odgaard, A., 1995, A New Method to Determine Trabecular Bone Elastic Properties and Loading Using Micromechanical Finite-Element Models, *J. Biomech.*, Vol. 28, No. 1, pp. 69-81.
- Weinans, H., Huiskes, R., and Grootenboer, H. J., 1992, The Behavior of Adaptive Bone-Remodeling Simulation Models, *J. Biomech.*, Vol. 25, No. 12, pp. 1425-1441.